ORIGINAL PAPER

Characterisation of contact twinning for cerussite, PbCO₃, by single-crystal NMR spectroscopy

Otto E. O. Zeman[1] · Jennifer Steinadler[1] · Rupert Hochleitner[2] · Thomas Bräuniger[1]

Abstract

Cerussite, PbCO₃, like all members of the aragonite group, shows a tendency to form twins, due to high pseudo-symmetry within the crystal structure. We here demonstrate that the twin law of a cerussite contact twin may be established using only ^{207}Pb-NMR spectroscopy. This is achieved by a global fit of several sets of orientation-dependent spectra acquired from the twin specimen, allowing to determine the relative orientation of the twin domains. Also, the full ^{207}Pb chemical shift tensor in cerussite at room temperature is determined from these data, with the eigenvalues being $\delta_{11} = (-2315 \pm 1)$ ppm, $\delta_{22} = (-2492 \pm 3)$ ppm, and $\delta_{33} = (-3071 \pm 3)$ ppm.

Keywords Cerussite · Twinning · ^{207}Pb-NMR · Chemical shift tensor

Introduction

Cerussite, PbCO₃, is a secondary mineral found in the oxidised zone of lead deposits, and crystallises in the aragonite structure type, usually described using the orthorhombic space group *Pmcn* (No. 62), see e.g. Antao and Hassan (2009). In Fig. 1, a single crystal specimen of cerussite from Tsumeb (Namibia), and a projection of the unit cell are shown.

Although natural single crystals may be found in mineral deposits of cerussite, its propensity to form twins has long been known. Early in the 20th century, Hubrecht (1904) reported "On cerussite multiples from Sardinia", and a similar account for findings in a Mexican mine was published by Hunt and Van Horn (1911). Indeed, twinning is commonly observed for all members of the aragonite family, due to the pseudo-symmetry inherent in the structure (Follner 1987; Makovicky 2012; Marzouki et al. 2015).

In the current work, cerussite is studied using Nuclear Magnetic Resonance (NMR) spectroscopy. NMR spectroscopy of single crystals, while labour-intensive, is generally

accepted to be the most precise method to establish NMR interaction parameters of a given nuclide in a solid sample (Vosegaard 2021). Also, as will be explained in detail below, using a single crystal instead of the more commonly used polycrystalline samples, spectral resolution is regained. The superior resolution of single-crystal NMR is exploited in many areas of basic research, including superconductors (Reichardt et al. 2018), ferromagnetism (Kitagawa et al. 2011) and high-pressure minerals (Grüninger et al. 2020). When investigating crystals by NMR spectroscopy, the measurements may also include twinned species, either on purpose (Reichardt et al. 2018) or inadvertently (Kitagawa et al. 2011; Mulla-Osman et al. 2001; Vosegaard et al. 1998). In some instances, it was even possible to establish the twin law of the investigated specimen using magnetic resonance data only (Mulla-Osman et al. 2001; Vosegaard et al. 1998). While the method of choice for quantifying twinning is X-ray diffraction (see, for example, Vinet et al. (2011)), it may be useful to have alternative methods available for crystals which are very large and/or contain heavy elements, leading to a high absorption factor, which makes diffraction analysis by standard laboratory equipment impossible.

In the current work, we have determined the full chemical shift tensor of ^{207}Pb in the cerussite structure from both single crystal and twinned samples. To properly analyse the NMR spectra from the two-domain twin species, the relative orientation of the two domains needs to be known. As described below, this information could be derived from

✉ Thomas Bräuniger
thomas.braeuniger@cup.lmu.de

1 Department of Chemistry, University of Munich (LMU), Butenandtstr. 5–13, 81377 Munich, Germany

2 Mineralogical State Collection Munich (SNSB), Theresienstr. 41, 80333 Munich, Germany
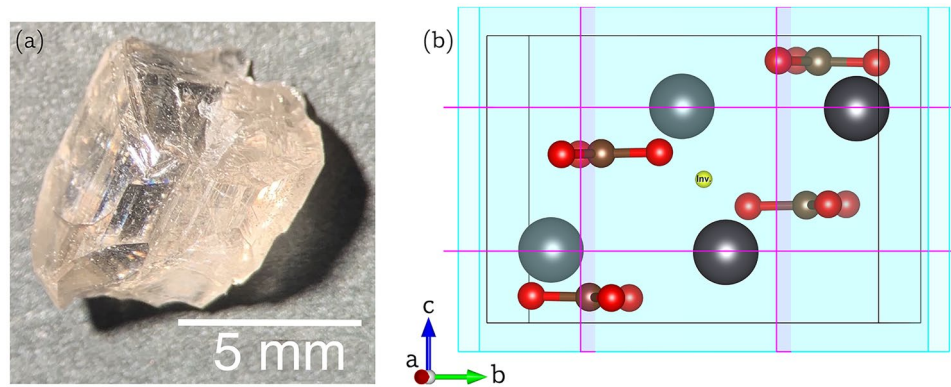
Fig. 1 **a** Single crystal of cerussite, PbCO$_3$, from Tsumeb, Namibia (Mineralogical state collection Munich, inventory MSM 34393). **b** Unit cell of cerussite in *Pmcn* setting, according to Antao and Hassan (2009). The four lead atoms at Wyckoff position 4*c* are shown in grey. They are located on mirror planes ($\frac{1}{4},y,z$; $\frac{3}{4},y,z$, shown in light blue), and pair-wise related by glide planes (shown in purple): *c* glides ($x,\frac{1}{4},z$; $x,\frac{3}{4},z$), and *n* glides ($x,y,\frac{1}{4}$; $x,y,\frac{3}{4}$). The carbon atoms (brown) are located on the same mirror planes as the lead atoms, with their covalent bonds to oxygen (red) in trigonal-planar coordination also shown. (Drawing generated with the VESTA program, Momma and Izumi (2011))

NMR data only, using a strategy that is widely applicable. With the knowledge about the relative domain orientations, the twin law of our twin specimen could be established. Before discussing our results in detail, the principles underlying ^{207}Pb-NMR in the solid state will be briefly reviewed.

Solid-state ^{207}Pb-NMR spectroscopy of cerussite

The information available from NMR spectroscopy of periodic inorganic structures is mostly complementary to those obtained from X-ray diffraction (XRD), but may be very useful. Whereas from XRD data of single crystals, the nature of the unit cell, and in particular, the asymmetric unit can in most cases be unequivocally derived, this task is more complex when dealing with diffraction data of a polycrystalline sample. Analysis of such powder XRD patterns can greatly benefit from knowing the exact number of crystallographic inequivalent atoms in the unit cell. This number may be obtained by simply counting the NMR resonances of a powder sample, see for example Martineau et al. (2014). In the aragonite structure of cerussite, the lead atoms are occupying Wyckoff position 4*c* (Sahl 1974; Chevrier et al. 1992; Antao and Hassan 2009). From one crystallographically independent lead site in the asymmetric unit, the symmetry elements of the unit cell generate four lead atoms overall (which may be referred to as "crystallographically equivalent"), as shown in Fig. 1b. To establish the number of crystallographically independent lead atoms by NMR, a ^{207}Pb-NMR spectrum of a polycrystalline sample of PbCO$_3$ under static conditions may be acquired, such as the one shown in Fig. 2a.

The broadness of this resonance reflects the fact that in solids, the NMR interaction parameters are generally orientation dependent. For ^{207}Pb with spin $I = 1/2$, the relevant interaction is the chemical shift (CS), and the wide line is a superposition of the many contributions of individual small crystallites. In a sufficiently large powder sample, all orientations are present simultaneously, each with a specific resonance frequency. The ^{207}Pb-NMR spectrum in Fig. 2a is consistent with the existence of only one crystallographically independent lead atom in the unit cell of cerussite, in agreement with the findings of XRD studies. NMR spectra of static powders become however difficult to analyse when the asymmetric unit contains several sites for one nuclide, and their respective spectral contributions overlap. This lack of resolution can be alleviated by application of the magic-angle-spinning (MAS) technique (Andrew 1981), with a ^{207}Pb-NMR spectrum of a powder sample of cerussite under MAS displayed in Fig. 2b. Here, the MAS is not fast enough to fully average the large chemical shift anisotropy of ^{207}Pb, and consequently, a manifold of so-called spinning side bands (SSB's) appears in the spectrum. For cerussite, this SSB manifold contains only one isotropic peak (which does not change position when the spinning speed is changed), again consistent with having a single lead atom in the asymmetric unit.

The situation is different when taking the NMR spectrum of a single crystal. In Fig. 2c, it may be seen that the ^{207}Pb-NMR spectrum of a cerussite single crystal shows *two* resonances. The powder spectrum in Fig. 2a is thus composed of individual crystallite contributions with two resonances each, but this information is lost in the superposition of all orientations. Generally, therefore, using single crystals instead of polycrystalline samples is a useful strategy to
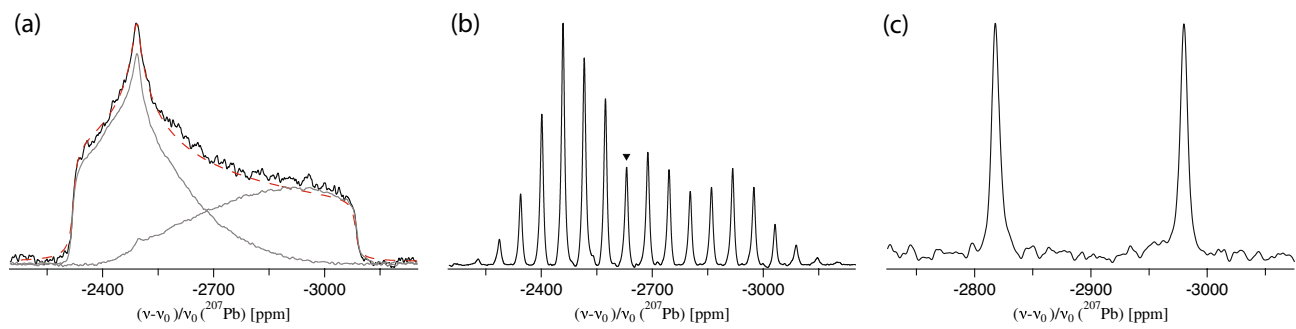
Fig. 2 **a** ^{207}Pb static powder spectrum of cerussite, PbCO$_3$, showing one crystallographic lead position. Due to the limited excitation length of the applied echo-sequence, the spectrum is a combination of two spectra (shown in grey) with the irradiation frequency offset located at the two edges of the static powder line, i.e. at −2320 ppm and −3090 ppm. The red, dashed line was calculated with the SIMPSON package (Bak et al. 2000), using the chemical shift values listed in Table 2 (right). **b** ^{207}Pb magic-angle spinning NMR spectrum of polycrystalline cerussite, acquired at 6 kHz spinning speed. The single isotropic band is indicated at −2630.4 ppm. **c** Static ^{207}Pb NMR spectrum of a single crystal of cerussite, showing two magnetically inequivalent lead positions. All spectra were acquired in a magnetic field of $\mathbf{B}_0 = 11.7$ T, and are plotted with the same maximum intensity, hence do not represent the true intensity variation between those three measurement conditions

regain spectral resolution. For example, Grüninger et al. (2020) recently investigated small single crystals of hydrous ringwoodite to resolve individual proton resonances. Coming back to cerussite, there is an apparent contradiction between having only one crystallographic independent lead atom in the unit cell, and observing two ^{207}Pb-NMR resonances in the spectrum in Fig. 2c. This is due to the fact that for single-crystal NMR, the number of observable NMR resonances for a given nuclide is *not* equal to the number of atoms in the asymmetric unit. Here, the concept of crystallographic equivalence is superseded by the stricter concept of magnetic equivalence, which states that only atoms connected by translation or inversion are equivalent in the NMR spectrum (the stringent condition being that the operator of the symmetry element must commute with the relevant spin Hamiltonian). Thus, two of the lead atoms at Wyckoff position 4c are situated on a mirror plane at $\left(\frac{1}{4}, y, z\right)$, and two on another mirror plane at $\left(\frac{3}{4}, y, z\right)$. The inversion center in the unit cell renders them pair-wise magnetically equivalent (along approximate diagonals in the projection of Fig. 1b), with the two members of each pair sitting on separate mirror planes. Therefore, two resonances are indeed expected in the ^{207}Pb-NMR spectrum of a single crystal of cerussite.

In Fig. 3, ^{207}Pb-NMR spectra for a limited number of crystal orientations are shown. All spectra are composed of two ^{207}Pb resonances with similar shape and intensity, with the resonance position markedly dependent on the crystal orientation with respect to the direction of the external magnetic field $\mathbf{B}_0$. These orientations are defined by a rotation angle φ around a goniometer axis, which in our case is perpendicular to $\mathbf{B}_0$, due to the architecture of the goniometer probe. Plots of the orientation dependence over the full range of $\varphi = 0^\circ \ldots 180^\circ$ are shown on the right of Fig. 3. From

those so-called rotation patterns, it is obvious that the positions of the resonance positions follow harmonic functions, which encapsulate information about the ^{207}Pb chemical shift tensor, δ_{Pb}. In the coordinate system of the spectrometer (sometimes referred to as *LAB* frame, where the z axis is parallel to $\mathbf{B}_0$), we thus measure spectra of a CS tensor which is being rotated step-wise in the static field by the goniometer mechanics. A useful alternative description is to choose the normalised orthorhombic crystal (*CRY*) coordinate system abc as a reference frame, since tensors expressed in this frame have a direct relation to the charge distribution in the unit cell. In the *CRY* frame, the CS tensor δ_{Pb}^{CRY} is stationary, but the orientation of the magnetic field (expressed by the normalised vector $\mathbf{b}_0$) is now a function of the rotation angle φ. For this situation, the general form of the harmonic functions shown in Fig. 3 may be written as (Volkoff et al. 1952; Weil and Anderson 1958):

$$\nu^{Pb}(\varphi)/\nu_0 = \mathbf{b}_0^T(\varphi) \cdot \delta_{Pb}^{CRY} \cdot \mathbf{b}_0(\varphi) = A + B\cos 2\varphi + C\sin 2\varphi \tag{1}$$

Here, ν_0 is the NMR reference frequency, and the factors A, B, and C are linear combinations of the CS tensor components, with their exact form depending on the orientation of the goniometer axis $\mathbf{g}$ in the *CRY* frame. When knowing $\mathbf{g}$, therefore, it is possible to determine δ_{Pb}^{CRY} by obtaining the A, B, C factors from fitting a sufficient number of experimental harmonics. The standard procedure in single-crystal NMR is to derive the orientation of the goniometer axis by additional methods, usually X-ray diffraction, and to use this prior knowledge in the analysis of the NMR data (Volkoff et al. 1952; Vosegaard 2021). It is however also possible to use the orientation of $\mathbf{g}$ as an additional variable in the data fit, and to thus determine it from NMR data only (Zeman et al. 2018, 2019a, b). Obviously, this is a useful strategy
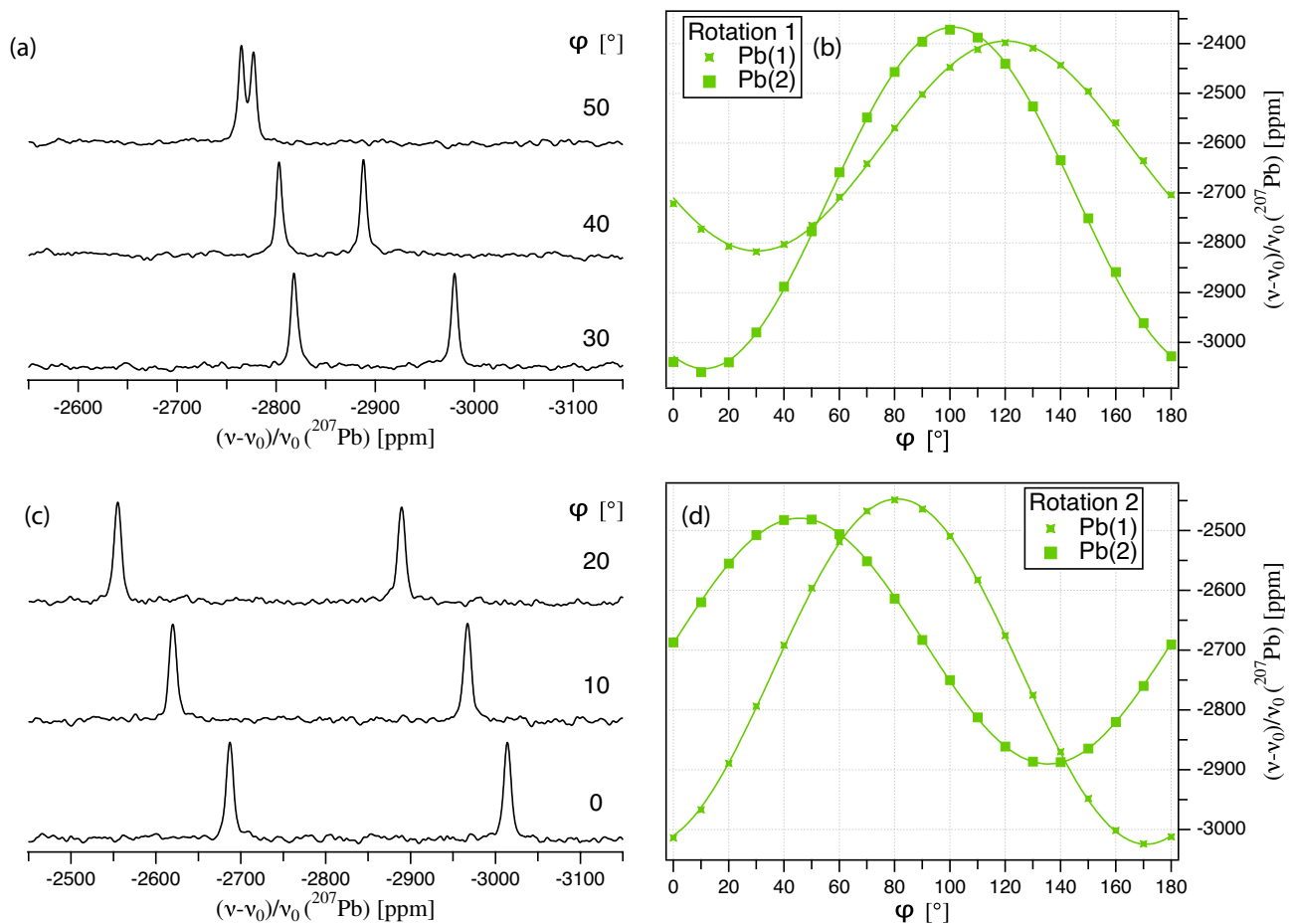
Fig. 3 ^{207}Pb-NMR spectra of the single crystal of cerussite, PbCO$_3$, depicted in Fig. 1a. The crystal was rotated counter-clockwise by the indicated angle φ around the rotation axis $\mathbf{g}_1$ (**a**) and $\mathbf{g}_2$ (**c**), both perpendicular to the external magnetic field $\mathbf{B}_0$. Full rotation pattern over 180° for the two magnetically inequivalent ^{207}Pb at Wyckoff position 4c, acquired by rotating the cerussite crystal step-wise by 10° around two goniometer axes $\mathbf{g}_1$ (**b**) and $\mathbf{g}_2$ (**d**). The lines represent the fit of the experimental points to the CS tensor elements and axis orientation (see text for details)

when XRD analysis is difficult because of large crystal size and/or presence of heavy elements such as lead, leading to a high absorption coefficient. To include the goniometer axis into the data fit, the following function is introduced to describe the motion of the magnetic field vector in the *CRY* frame:

$$\mathbf{b}_0(\varphi) = \mathbf{v} \sin\left(\varphi - \varphi_\Delta\right) + \mathbf{u} \cos\left(\varphi - \varphi_\Delta\right) \tag{2}$$

Here, $\mathbf{v}$ and $\mathbf{u}$ are two auxiliary unit vectors in a plane perpendicular to the goniometer axis. These vectors are conveniently generated from $\mathbf{g}$ by choosing a reference vector which is non-parallel to $\mathbf{g}$, the definition of which determines the offset angle φ_Δ. If the unit vector along the crystallographic *c*-axis is chosen as reference (other choices are possible), $\mathbf{v}$ and $\mathbf{u}$ are calculated by:

$$\mathbf{v} = \frac{1}{\sin\theta_g}(\mathbf{g} \times \mathbf{c}); \qquad \mathbf{u} = \mathbf{v} \times \mathbf{g} = \frac{1}{\sin\theta_g}\left(\mathbf{c} - \mathbf{g}\cos\theta_g\right) \tag{3}$$

The above equations are the route by which the goniometer axis orientation (described by the spherical coordinates θ_g and ϕ_g) is entered as a variable into the fit equations, and may be extracted by simultaneous fit together with the tensor components. Further technical details about this global fit procedure, which may also applied to determine tensors other than that of the chemical shift (such as EFG or dipolar coupling) may be found in Zeman et al. (2018, 2019a, b). In the context of the current work, the capability to establish the goniometer axis orientation from NMR data only is essential for determining the twin law of a twinned specimen, as described below.

Materials and methods

All NMR spectra were acquired on a BRUKER AVANCE-III 500 spectrometer at LMU Munich, with the Larmor frequency being $\nu_0(^{207}\text{Pb}) = 104.63$ MHz, using echo acquisition to minimize base line roll (Kunwar et al. 1986), and a recycle delay of 16 s. Single-crystal ^{207}Pb-NMR spectra were acquired at room temperature on a commercial wide-bore BRUKER static NMR probe, equipped with a home-build 6 mm solenoid coil, using echo pulses of 2 and 4 μs duration. Orientation change was realised with a clip-on goniometer build by NMR Service GmbH (Erfurt, Germany), which allows for defined rotations in steps of 10 degrees. A polycrystalline sample was prepared by crushing single crystals of cerussite with an agate mortar, and measured using a 4 mm rotor under both MAS and static conditions, employing echo pulse durations of 5.25 and 10.5 μs. All spectra were referenced indirectly to ^{1}H in 100% TMS at -0.1240 ppm, which is equivalent to the common reference of $\text{Pb(NO}_3)_2$ powder at -3487.5 ppm. The global fit of the rotation pattern, including the orientation of the goniometer axis in the crystal frame, was performed with the WaveMetrics Inc. program IGOR PRO 7.08.

Results

Determination of the twin law

In Fig. 4, a ^{207}Pb NMR spectrum of a cerussite twin specimen (originating from the same location as the single crystal pictured in Fig. 1a) is shown, before cutting it into a larger and smaller piece, the spectra of which are also displayed. In contrast to the single-crystal spectra shown in Fig. 3 and discussed above, the twin specimen shows four signals in each spectrum, forming two pairs of equal intensity. The pairs of equal intensity belong to two twin domains, which we will label A and B, respectively. The upper spectrum in Fig. 4 belongs to the original twin crystal (weighing 276 mg), where the ^{207}Pb-NMR intensity ratio of $B : A = 1 : 9.8$ gives a good estimate of the relative twin domain sizes. The middle spectrum in Fig. 4 belongs to the larger piece after cutting, with a remaining weight of 190 mg, the bottom spectrum to the smaller piece weighing 86 mg. In both these spectra, the ratio of $B : A$ is significantly changed in comparison to the original twin, with the larger crystal containing mostly domain A, with $B : A = 1 : 17.1$, and the smaller piece having a higher proportion of domain B, with $B : A = 1 : 2.1$. Such changes in relative domain sizes induced by cutting can only occur for
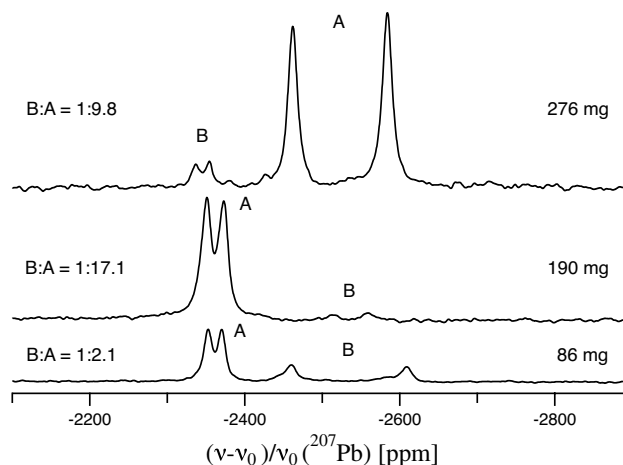
Fig. 4 Static ^{207}Pb NMR spectrum of a twinned crystal of cerussite (top). Spectra after cutting the original crystal into a larger (middle) and smaller piece (bottom), with the respective weights of all crystals listed on the right. On the left of the spectra, the relative spectral contributions of the two twin domains A and B are indicated, showing that the ratio of A to B is changing. The spectra have been acquired with a differing number of scans, with the plotted intensity scaled according to crystal weight. For all spectra, the orientation of the crystals in the magnetic field has been chosen such that all four resonances are resolved

crystals with distinct twin domains, since for intergrowth twinning, as for example exhibited by cinnabar (Termier 1897), the relative contributions of the two domains would obviously be identical for any chosen part of the crystal.

For the twin crystal with a weight of 86 mg, the resonances of the smaller B domain are clearly discernible in the ^{207}Pb NMR spectrum, and they can be easily separated from the A domain signals by their smaller signal intensity, as may be seen in Fig. 5a, with a full rotation pattern of the twin shown in Fig. 5b. As explained above, the harmonic functions connecting the resonance positions in rotation patterns may be used to determine NMR interaction tensors, plus the orientation of the goniometer axis. It is important to realise that the data points collected for the domains A and B by rotating a twin specimen around a common goniometer axis could have been also recorded by rotating two separate crystals around the axes $\mathbf{g}_A$ and $\mathbf{g}_B$. Thus, by performing a global fit (Zeman et al. 2018, 2019a, b) of the NMR data shown in Fig. 5b, the orientation of $\mathbf{g}_A$ for domain A, and that of $\mathbf{g}_B$ for domain B were obtained, and are listed in Table 1. In the common crystal frame CRY, the vectors $\mathbf{g}_A$ and $\mathbf{g}_B$ obviously possess different directions, since they belong to two distinct domains of the twin. By switching the point of view to the (LAB) frame of the goniometer, where only one physical rotation axis exists, it can be understood that the difference between $\mathbf{g}_A$ and $\mathbf{g}_B$ actually represents the orientation difference of the two crystal frames belonging to the
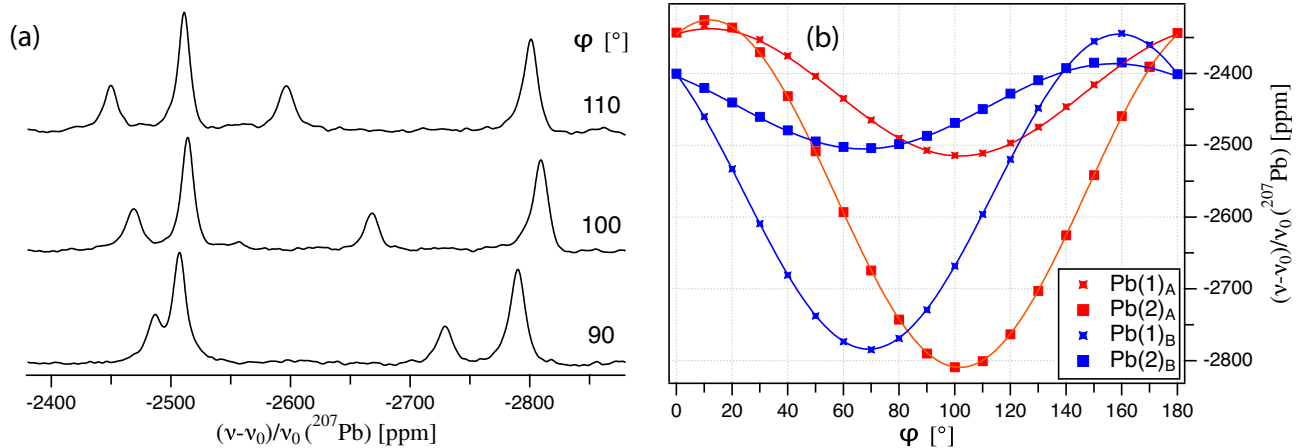
Fig. 5 a ^{207}Pb NMR spectra of a twinned cerussite crystal rotated counter-clockwise by the indicated angle φ around a rotation axis perpendicular to the external magnetic field $\mathbf{B}_0$. **b** Full rotation pattern over 180° for the two magnetically inequivalent ^{207}Pb at Wyckoff position 4c in each twin-crystal domain A (red) and B (blue), acquired by rotating the cerussite twin step-wise by 10° around one goniometer axis. The lines represent the fit of the experimental points to the CS tensor elements and axis orientation (see text for details)

Table 1 Orientation of the various goniometer axes $\mathbf{g}_i$ used for the determination of the ^{207}Pb CS tensor of cerussite, PbCO$_3$, from a global fit of the the indicated rotation patterns

Goniometer axis (rotation pattern)	θ_g	ϕ_g	φ_Δ
$\mathbf{g}_1$ (Fig. 3b)	$(136.3 \pm 0.3)°$	$(142.6 \pm 0.3)°$	$(142.4 \pm 0.2)°$
$\mathbf{g}_2$ (Fig. 3d)	$(112.2 \pm 0.4)°$	$(205.1 \pm 0.3)°$	$(51.6 \pm 0.1)°$
$\mathbf{g}_A$ (Fig. 5b)	$(118.5 \pm 0.2)°$	$(78.5 \pm 0.4)°$	$(113.4 \pm 0.4)°$
$\mathbf{g}_B$ (Fig. 5b)	$(66.3 \pm 0.1)°$	$(70.0 \pm 0.2)°$	$(48.7 \pm 0.3)°$

The directions of the $\mathbf{g}_i$ are given in spherical coordinates (θ_g, ϕ_g) of the *CRY* frame, with the errors reflecting the fit residuals. The φ_Δ parameters define the starting point of each rotation

domains A and B, which is the twin law we seek. Unfortunately, to relate one twin frame to another, three Euler angles (or directional cosines) are needed, and the difference of two vectors provides only two of those. Fortunately, it is well documented that the most common type of twinning in cerussite is contact twinning, predominantly occurring in the form of {110} and {130} twins (Hubrecht 1904; Hunt and Van Horn 1911; Pogue 1913; Franke and Lenk 1981; Follner 1987; Cook 1997). In case of such a simple cerussite contact twin, the contact plane of the twin domains is a mirror plane containing the crystallographic c-axis. Since this mirror plane also relates our two goniometer axes $\mathbf{g}_A$ and $\mathbf{g}_B$ to each other by mirror symmetry, the twin contact plane is fully defined by the bisector of $\mathbf{g}_A$ and $\mathbf{g}_B$, and the c-axis in the *CRY* frame. For our cerussite twin, the bisector between $\mathbf{g}_A$ and $\mathbf{g}_B$ points along $(1\,3\,0)^T$ with a deviation of 3.5°. It is therefore highly likely that the investigated cerussite crystal is a {130} contact twin, one of the two twin types already known to Hubrecht (1904). It should however be noted that

due to the bisector deviation of 3.5°, our NMR results do not allow us to unambiguously distinguish between {130} and very similar twinning planes, e.g. the {270} plane.

As already mentioned, twin laws have been derived from magnetic resonance data of single crystals before, see for example Mulla-Osman et al. (2001), or Vosegaard et al. (1998). In the latter study, ^{71}Ga spectra of a synthetic twin of β-Ga$_2$O$_3$ were recorded and analysed. The actual derivation of the twin law by Vosegaard et al. (1998) relied on a special crystallographic situation: The two gallium atoms in the asymmetric unit are located on mirror planes, imposing symmetry restriction on the tensor components. Similarly, in the ^{35}Cl-NMR study of tetramethylammonium cadmium chloride by Mulla-Osman et al. (2001), the elucidation of the relative domain orientation was built on the presence of a sixfold symmetry axis. In contrast, the approach demonstrated here, namely the determination of individual goniometer axes orientations for the respective domains in their common crystal frame, works in a more general way. Whenever applicable, this method will provide information about relative domain orientation, even though it might be incomplete, as in the case of cerussite, where additional crystallographic information was needed to fix the third Euler angle relating the two domain frames.

Determination of the ^{207}Pb chemical shift tensor

The systematic recording of the orientation dependence of the ^{207}Pb-NMR resonances, as shown in Figs. 3 and 5, allows the determination of the full ^{207}Pb chemical shift (CS) tensor in cerussite. The two magnetically inequivalent lead sites in cerussite can be considered to be related by a 180° rotation about the crystallographic c-axis and are

situated on mirror planes parallel to the *bc* plane. These symmetry requirements affect the structure of the [207] Pb chemical shift tensors in the *CRY* frame. With CS tensors commonly expressed as 3×3 symmetric matrices (Anet and O'Leary 1991), the general forms of the [207] Pb CS tensors in cerussite are given by:

$$\delta_{Pb(1)}^{CRY} = \begin{pmatrix} P & 0 & 0 \\ 0 & Q & R \\ 0 & R & S \end{pmatrix} \quad \overset{180^{\circ}_{c}}{\longleftrightarrow} \quad \delta_{Pb(2)}^{CRY} = \begin{pmatrix} P & 0 & 0 \\ 0 & Q & -R \\ 0 & -R & S \end{pmatrix}$$
$$(x, \frac{1}{4}, z) \qquad\qquad (\bar{x}+\frac{1}{2}, \frac{3}{4}, z+\frac{1}{2})$$
(4)

To determine the tensor components *P*, *Q*, *R*, and *S* and the orientation of the rotation axis from the respective rotation patterns in Figs. 3 and 5, we largely follow the approach extensively described before for orthorhombic $PbSO_4$ (Zeman et al. 2019a). Thus, the two rotation patterns for the cerussite single crystal with the rotation axis $\mathbf{g}_1$ (Fig. 3b) and $\mathbf{g}_2$ (Fig. 3d), as well as the rotation pattern of the twinned cerussite (Fig. 5b) with rotation axes $\mathbf{g}_A$ and $\mathbf{g}_B$, corresponding to an individual rotation of each twin domain, were simultaneously fitted according to Eq. 1. The fit converged on a global solution, with the resulting rotation (goniometer) axes listed in Table 1, and the following [207] Pb chemical shift tensor components, with the errors reflecting the fit residuals:

$$P = (-2315 \pm 1) \text{ ppm} \quad Q = (-3012 \pm 3) \text{ ppm}$$
$$R = (173.1 \pm 0.5) \text{ ppm} \quad S = (-2550 \pm 1) \text{ ppm}$$
(5)

The CS tensor defined by the *P*, *Q*, *R*, *S* values in the *CRY* frame can be transformed into its principal axes system (*PAS*) by diagonalisation, resulting in the eigenvalues and eigenvectors listed in Table 2 (left). The weighted sum of these diagonal tensor elements is the isotropic chemical shift, $\delta_{iso} = \frac{1}{3}(\delta_{11} + \delta_{22} + \delta_{33})$. From our [207] Pb CS tensor values for cerussite, the isotropic shift computes to $\delta_{iso} = (-2626 \pm 3)$ ppm.

Information about the magnitude of the CS tensor may also be extracted from a polycrystalline sample, using either static or magic-angle spinning (MAS) NMR spectroscopy. Therefore, we acquired 207Pb-NMR spectra of a sample of cerussite crushed into a powder at three different MAS spinning speeds, namely 10 kHz, 8 kHz, and 6 kHz, with the latter shown in Fig. 2b. It is well known that [207] Pb chemical shifts vary strongly with temperature for many inorganic compounds, and even friction heating from MAS (Milder et al. 1995) may lead to a noticeable change in the isotropic chemical shift. Extrapolating δ_{iso} over the squared MAS frequency (see for example Zeman et al. (2019a) for an illustration of this procedure) allows the determination of the isotropic shift at room temperature to $\delta_{iso}^{MAS} = (-2632 \pm 5)$ ppm. Within error limits, this is identical to the value derived from single-crystal NMR. To also extract the three eigenvalues

Table 2 207Pb chemical shift tensor δ^{CRY} of cerussite, $PbCO_3$

	Single-crystal NMR	MAS NMR	Static powder NMR
δ_{11}^{PAS}	(-2315 ± 1) ppm	(-2324 ± 4) ppm	(-2320 ± 7) ppm
δ_{22}^{PAS}	(-2492 ± 3) ppm	(-2485 ± 3) ppm	(-2492 ± 4) ppm
δ_{33}^{PAS}	(-3071 ± 3) ppm	(-3082 ± 3) ppm	(-3084 ± 10) ppm
d_{11}	90.0°, 0.0°		
d_{22}	18.4°, 90.0°		
d_{33}	71.6°, 270.0°		
δ_{iso}		(-2630 ± 3) ppm	
	(-2626 ± 3) ppm	(-2632 ± 5) ppm[a]	(-2632 ± 7) ppm

Left: determined from room temperature single-crystal NMR experiments about the four rotation axes listed in Table 1. The orientation of the corresponding eigenvectors is given in spherical coordinates (θ, φ) in the normalised orthorhombic *abc* crystal system, and refer to the atom closest to the origin, i.e. Pb(1). The error values are derived from the fit residuals. Middle: determined from an analysis according to Herzfeld and Berger (1980) of the rotational side band pattern at $\nu_r = +6$ kHz MAS (i.e., at slightly elevated temperature), using the *hba 1.7.5* program (Eichele 2015), leading to $\rho = 0.58 \pm 0.01$ and $\mu = 13.2 \pm 0.1$. The error values of the tensor components are derived from those of ρ and μ. Right: determined from a static polycrystalline powder sample at room temperature. Error values of tensor components are derived from a SIMPSON (Bak et al. 2000) simulation

[a] From extrapolation of squared MAS frequencies to zero spinning

of the CS tensor, the MAS spectrum at 6 kHz was analysed according to Herzfeld and Berger (1980), with the results listed in Table 2 (middle). Finally, the chemical shift eigenvalues were also estimated from the static [207] Pb powder spectrum shown in Fig. 2a. This spectrum was compared to various spectra calculated with the SIMPSON package (Bak et al. 2000), with the best agreement between the experiment and simulation found for the eigenvalues listed in Table 2 (right). Overall, the tensor eigenvalues derived from different methods agree well with each other and also with those previously reported from static spectra of a polycrystalline sample by Neue et al. (1996).

Conclusion

The mineral cerussite, $PbCO_3$, similar to other members of the aragonite group, is known to form pseudo-hexagonal contact twins, as a result of high pseudo-symmetry within the individual crystal structures. In this work, we have shown that solid-state NMR spectroscopy may successfully be employed to quantitatively characterise such crystal twinning. This was achieved by a global fit of several sets of orientation-dependent [207] Pb-NMR spectra acquired from a twin specimen, from which the relative orientation of the twin domains could be derived. In addition, the full [207] Pb chemical shift tensor in cerussite at room temperature was determined from these data.

The approach to characterise crystal morphology by NMR spectroscopy can be extended to even larger crystal agglomerates, as recently demonstrated in a NMR study of mimetite and related apatites (Zeman et al. 2021).

Declarations

References

Andrew ER (1981) Magic angle spinning in solid state n.m.r. spectroscopy. Philos Trans Royal Soc A 299:505–520

Anet FAL, O'Leary DJ (1991) The shielding tensor part: I understanding its symmetry properties. Concepts Magn Reson 3:193–214

Antao SM, Hassan I (2009) The orthorhombic structure of $CaCO_3$, $SrCO_3$, $PbCO_3$ and $BaCO_3$: linear structural trends. Canad Mineral 47:1245–1255

Bak M, Rasmussen JT, Nielsen NC (2000) SIMPSON: a general simulation program for solid-state NMR spectroscopy. J Magn Reson 147:296–330

Chevrier G, Giester G, Heger G, Jarosch D, Wildner M, Zemann J (1992) Neutron single-crystal refinement of cerussite, $PbCO_3$, and comparison with other aragonite-type carbonates. Z Kristallogr 199:67–74

Cook RB (1997) Connoisseur's choice: cerussite, tsumeb. Namibia. Rocks Miner 72(3):176–180

Eichele K (2015) HBA 1.7.5. Universität Tübingen, Tübingen

Follner H (1987) Twin laws explained by partitions of space. Cryst Res Technol 22(4):509–516

Franke W, Lenk K (1981) The morphology of cerussite $PbCO_3$ grown in silica gel and on hydrothermal conditions. J Cryst Growth 51:309–313

Grüninger H, Liu Z, Brauckmann O, Fei H, Ballaran TB, Martin T, Siegel R, Kentgens APM, Frost DJ, Senker J (2020) Hydroxyl defects and oxide vacancies within ringwoodite—toward understanding the defect chemistry of spinel-type Oxides. J Phys Chem C 124:12001–12009

Herzfeld J, Berger AE (1980) Sideband intensities in NMR spectra of samples spinning at the magic angle. J Chem Phys 73:6021–6030

Hubrecht PF (1904) On cerussite multiples from Sardinia. Z Kryst Miner 40:147–188

Hunt WF, Van Horn FR (1911) Cerussite twins from the begona mine, Cerro de San Pedro, San Luis Potosi, Mexico. Am J Sci 32:45–47

Kitagawa K, Mezaki Y, Matsubayashi K, Uwatoko Y, Takigawa M (2011) Crossover from commensurate to incommensurate antiferromagnetism in stoichiometric NaFeAS revealed by single-Crystal ^{23}Na, ^{75}As-NMR experiments. J Phys Soc Japan 80:033705

Kunwar AC, Turner GL, Oldfield E (1986) Solid-state spin-echo Fourier transform NMR of ^{39}K and ^{67}Zn salts at high field. J Magn Reson 69:124–127

Makovicky E (2012) Twinning of aragonite—the OD approach. Miner Petrol 106:19–24

Marzouki MA, Souvignier B, Nespolo M (2015) Twinning of aragonite—the crystallographic orbit and sectional layer group approach. Acta Crystallogr A 71:195–202

Martineau C, Senker J, Taulelle F (2014) NMR crystallography. Annu Rep NMR Spectro 82:1–57

Milder T, Ernst H, Freude D (1995) ^{207}Pb NMR detection of spinning-induced temperature gradients in MAS rotors. Solid State Nucl Magn Reson 5(3):269–271

Momma K, Izumi F (2011) VESTA 3 for three-dimensional visualization of crystal, volumetric and morphology data. J Appl Cryst 44:1272–1276

Mulla-Osman S, Michel D, Völkel G, Peral I, Madariaga G (2001) ^{35}Cl NMR studies of the domain structure of tetramethylammonium cadmium chloride (TMCC) at lower temperatures. J Phys: Condens Matter 13:1119–1131

Neue G, Dybowski C, Smith ML, Hepp MA, Perry DL (1996) Determination of $^{207}Pb^{2+}$ chemical shift tensors from precise powder lineshape analysis. Solid State Nucl Magn Reson 6:241–250

Pogue JE (1913) On cerussite twins from the mammoth mine, Pinal county, Arizona. Amer Jour Sci 35:90–92

Reichardt S, Jurkutat M, Guehne R, Kohlrautz J, Erb A, Haase J (2018) Bulk charge ordering in the $extCuO_2$ plane of the cuprate superconductor $extYBa_2extCu_3extO_{6.9}$ by high-pressure NMR. Condens Matter 3:23

Sahl K (1974) Verfeinerung der Kristallstruktur von Cerussit, $PbCO_3$. Z Kristallogr 139:215–222

Termier P (1897) Cinnabar and Onofrite from Ouen-Shan-Tchiang China. Bull Soc Franc Min 20:204–210

Vinet N, Flemming RL, Higgins MD (2011) Crystal structure, mosaicity, and strain analysis of Hawaiian olivines using in situ X-ray diffraction. Am Mineral 96:486–497

Volkoff GM, Petch HE, Smellie DWL (1952) Nuclear electric quadrupole interactions in single crystals. Can J Phys 30:270–289

Vosegaard T, Byriel IP, Binet L, Massiot D, Jakobsen HJ (1998) Crystal structure studies by single-crystal NMR spectroscopy. ^{71}Ga and ^{69}Ga single-crystal NMR of β-Ga_2O_3 Twins. J Am Chem Soc 120:8184–8188

Vosegaard T (2021) Single-crystal NMR spectroscopy. Prog Nucl Magn Reson 123:51–72

Weil JA, Anderson JH (1958) Determination of the g tensor in paramagnetic resonance. J Chem Phys 28:864–866

Zeman OEO, Hoch C, Hochleitner R, Bräuniger T (2018) NMR interaction tensors of ^{51}V and ^{207}Pb in vanadinite, $Pb_5(VO_4)_3Cl$, determined from DFT calculations and single-crystal NMR measurements, using only one general rotation axis. Solid State Nucl Magn Reson 89:11–20

Zeman OEO, Steinadler J, Hochleitner R, Bräuniger T (2019a) Determination of the full ^{207}Pb chemical shift tensor of anglesite, $PbSO_4$, and correlation of the isotropic shift to lead-oxygen distance in natural minerals. Crystals 9(1):43

Zeman OEO, Steinadler J, Hochleitner R, Bräuniger T (2019b) Single-crystal ^{207}Pb-NMR of wulfenite, $PbMoO_4$, aided by simultaneous

measurement of phosgenite, $Pb_2 Cl_2 CO_3$. Solid State Nucl Magn Reson 103:17–24

Zeman OEO, Hochleitner R, Schmahl WW, Karaghiosoff K, Bräuniger T (2021) Relation between [207]Pb NMR chemical shift and the morphology and crystal structure for the apatites $Pb_5(AO_4)_3Cl$, vanadinite (A = V), pyromorphite (A = P), and mimetite (A = As). Amer Miner 106:541–548